

# PyRAD: assembly of *de novo* RADseq loci for phylogenetic analyses

Deren A. R. Eaton<sup>1,2</sup><sup>1</sup>Committee on Evolutionary Biology, University of Chicago, 1025 E. 57th St. Chicago, IL 60637, USA and <sup>2</sup>Botany Department, Field Museum of Natural History, 1400 S. Lake Shore Dr. Chicago, IL 60605, USA

Associate Editor: David Posada

## ABSTRACT

**Motivation:** Restriction-site-associated genomic markers are a powerful tool for investigating evolutionary questions at the population level, but are limited in their utility at deeper phylogenetic scales where fewer orthologous loci are typically recovered across disparate taxa. While this limitation stems in part from mutations to restriction recognition sites that disrupt data generation, an additional source of data loss comes from the failure to identify homology during bioinformatic analyses. Clustering methods that allow for lower similarity thresholds and the inclusion of indel variation will perform better at assembling RADseq loci at the phylogenetic scale.

**Results:** *PyRAD* is a pipeline to assemble *de novo* RADseq loci with the aim of optimizing coverage across phylogenetic datasets. It uses a wrapper around an alignment-clustering algorithm, which allows for indel variation within and between samples, as well as for incomplete overlap among reads (e.g. paired-end). Here I compare *PyRAD* with the program *Stacks* in their performance analyzing a simulated RADseq dataset that includes indel variation. Indels disrupt clustering of homologous loci in *Stacks* but not in *PyRAD*, such that the latter recovers more shared loci across disparate taxa. I show through re-analysis of an empirical RADseq dataset that indels are a common feature of such data, even at shallow phylogenetic scales. *PyRAD* uses parallel processing as well as an optional hierarchical clustering method, which allows it to rapidly assemble phylogenetic datasets with hundreds of sampled individuals.

**Availability:** Software is written in Python and freely available at <http://www.dereeneaton.com/software/>

**Contact:** [daeaton.chicago@gmail.com](mailto:daeaton.chicago@gmail.com)

**Supplementary Information:** Supplementary data are available at *Bioinformatics* online.

Received on December 16, 2013; revised on February 24, 2014; accepted on February 25, 2014

## 1 INTRODUCTION

Restriction-site-associated DNA libraries (RADseq; Baird *et al.*, 2008) and related genotyping-by-sequencing approaches (e.g. GBS, Etter *et al.*, 2011; ddRADseq, Peterson *et al.*, 2012) take advantage of next-generation sequencing platforms to generate short reads from thousands of potentially homologous loci, across multiple individuals, by targeting genomic regions adjacent to restriction enzyme cut sites. In contrast to whole-genome shotgun data, this provides a more efficient and economical source for performing comparisons across many sampled individuals, making it a popular tool for population genetic analyses

(reviewed in Narum *et al.*, 2013). The problem of efficiently obtaining sequence data across many individuals is also relevant to studies at deeper evolutionary time scales, such as genus- or family-level phylogenetics, and it is at this scale that RADseq is now receiving increased attention.

RAD sequences generated *in silico* from multi-species genome alignments have been shown to retain accurate phylogenetic information over evolutionary divergences as deep as 60 million years (Cariou *et al.*, 2013; Rubin *et al.*, 2012); however, to date, all empirical RADseq studies conducted above the species level were done at much shallower scales (Bergey *et al.*, 2013; Eaton and Ree, 2013; Jones *et al.*, 2013; Keller *et al.*, 2013; Lexer *et al.*, 2013; Nadeau *et al.*, 2013; Stölting *et al.*, 2013; The Heliconius Genome Consortium, 2012; Wagner *et al.*, 2013; Wang *et al.*, 2013). Still, these studies confirm theoretical expectations by demonstrating that concatenated, genome aligned or even individual RADseq loci are capable of recovering well-supported gene trees and species trees. Yet, these studies also demonstrate that large amounts of missing data are a common feature of RADseq, which may limit its applications.

Theoretically, the ultimate scale over which RADseq data will be recovered, and thus phylogenetically useful, is inherently limited by mutations that disrupt restriction recognition sites, causing ‘locus dropout’—manifest as more missing data between more distantly related samples. However, empirically such limits are approached much sooner owing to the loss of data to other technical factors related to data generation and analysis. For example, the choice of restriction enzyme, the size of selected fragments and variation in sequencing coverage across samples all affect the number of loci recovered. Moreover, bioinformatic analyses used to assemble RADseq datasets recover different amounts of data depending on the parameters used to identify and cluster orthologs as well as filter for paralogs (or repetitive DNA regions.) In this article, I focus mainly on the latter aspect of locus dropout: factors limiting the identification (recovery) of orthologous loci when they are present in a dataset.

Few programs are currently available to assemble RADseq data, which currently includes *Stacks* (Catchen *et al.*, 2011, 2013), *Rainbow* (Chong *et al.*, 2012) and *rtid* (Peterson *et al.*, 2012). Here I describe a new software pipeline called *PyRAD*, which assembles *de novo* aligned RADseq loci for population-level or phylogenetic analyses, with a particular focus on the analysis of highly divergent samples. *PyRAD* differs from both *Stacks* and *Rainbow* through its use of a global alignment clustering algorithm—performed with a wrapper around the program *USEARCH* (Edgar, 2010)—which allows for incorporation

of indel variation while identifying homology. In this way, *PyRAD* is more similar to *rtd*, which uses a graph clustering algorithm that also allows for indels. *PyRAD* stands apart from these programs in its speed, flexibility for analyzing multiple RADseq data types, its scalability to extremely large and divergent datasets and its ease of use. Below I describe the *PyRAD* pipeline in detail. I then demonstrate its performance on simulated and empirical datasets and compare the results with those of *Stacks*, which is currently the most commonly used alternative software.

## 2 METHODS

### 2.1 Summary of a *de novo* assembly

*PyRAD* requires as dependencies only the executable programs *USEARCH* (Edgar, 2010) and *MUSCLE* (Edgar, 2004), in addition to the common Python packages *Scipy* and *Numpy*. It runs on Mac and Linux, is accessed through a command-line interface and uses a modular framework with a full analysis composed of seven sequential steps:

- (1) De-multiplexing (separate by barcodes)
- (2) Quality filtering and removal of barcodes, cut sites and adapters
- (3) Clustering within samples and alignment
- (4) Joint estimation of error rate and heterozygosity
- (5) Consensus base calling and paralog detection
- (6) Clustering across samples
- (7) Alignment across samples, filtering and formatting

The de-multiplexing step (1) separates raw FASTQ formatted sequence data into separate files for each sample, allowing a user set maximum number of mismatches (errors) in a barcode. If samples are already de-multiplexed, this step can be skipped. Filtering (2) then removes barcodes and Illumina adapters, if present, and filters reads by their quality scores, replacing base calls below a user-set limit with an ambiguous base (N). Reads with more than a user-defined number of Ns are discarded. The clustering step (3) first collapses replicate sequences into individual records while retaining their total number of occurrences. Sequence order is randomized and clustering is performed using *USEARCH* with all heuristic options turned off. This creates clusters (stacks) by matching each sequential sequence to a 'seed' sequence that came before it, or else creating a new seed. The resulting stacks are aligned with *MUSCLE*.

The next step (4) uses the maximum likelihood equation of Lynch (2008) to jointly estimate the mean heterozygosity and sequencing error rate from the base frequencies at each site across all stacks in an individual (with greater than a set minimum depth of coverage), and uses these values (5) to calculate the binomial probability a site is homozygous (aa or bb) versus heterozygous (ab) (Li *et al.*, 2008). A base call is only made if the depth of coverage is above a user-set minimum, and high enough to make a statistical base call, else it is called undetermined (N). Consensus sequences containing more than a maximum number of undetermined sites are discarded. To filter for paralogs (or repetitive or high copy number DNA regions, hereafter referred to collectively as 'paralogs' for simplicity), consensus sequences are also discarded if they contain more than a maximum number of heterozygous sites or more than the allowed number of haplotypes (two for diploids).

Putative orthologs are then identified by clustering consensus loci across samples in *USEARCH*, using only one allele from each consensus sequence to measure sequence similarity, but retaining data for both (or multiple) alleles (6). The resulting stacks are aligned and filtered once again for paralogs before being output in a variety of familiar formats as individual or concatenated loci (e.g. Fasta, Phylip, Nexus), or in

several custom formats [e.g. Haplotypes, single nucleotide polymorphisms (SNPs) and unlinked SNPs] (7). The filter applied in this step makes use of a user-set maximum for the number of shared heterozygous sites across all samples in the dataset (maxSharedH). For a phylogenetic scale dataset the expectation for this number is unknown, but should be fairly low under the assumption that polymorphisms are less likely to be retained over deep divergences than are fixed differences between paralogs. Loci containing one or more heterozygous sites shared across more than 'maxSharedH' samples are thus discarded as potential paralogs. Step 7 can be repeated while substituting different subsets of taxa, and requiring different amounts of coverage across them, to construct datasets of varying size and completeness.

### 2.2 Hierarchical clustering for large datasets

As the size and scope of RADseq studies continue to grow, the computational time required to assemble datasets can become burdensome. In *PyRAD* the limiting step for large data is often among-sample clustering (step 5), which is not parallelized. Clustering time scales with the total number of unique stacks and studies with many samples (>100) can quickly accumulate many low coverage or singleton loci that greatly slow run times. To speed this step, an optional hierarchical clustering approach that splits the job into smaller parallelized units can be implemented. Here, loci are first clustered across samples within user-defined clades, with each clade using a separate processor. The seeds of these stacks are then used to cluster with seeds of stacks from other clades (Fig. 1) before a final stack is reconstructed from the matches to each seed from each hierarchical clustering step. A further gain in speed can be attained by excluding at each step loci that do not cluster with at least some minimum number of other samples, under the assumption that such loci are less likely to match with more distant relatives in the next step. Although this gain in speed comes at the cost of excluding loci with low taxon coverage, such loci are typically of little use in downstream analyses.

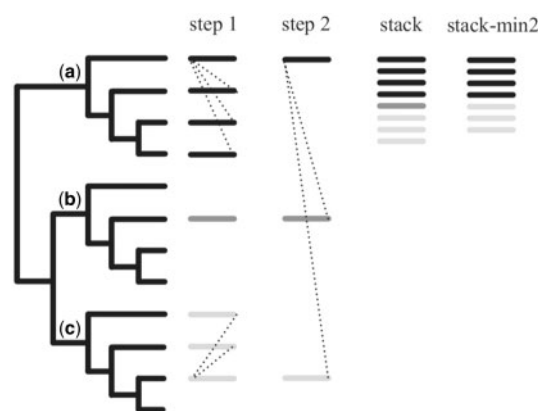


**Fig. 1.** Optional hierarchical clustering approach for fast across-sample clustering of large datasets in *PyRAD*. In the first iteration, clustering is performed among samples within each user-defined clade (a, b and c). Dotted lines show clustering of sequences to the randomly assigned seed sequence in each stack. In subsequent steps, the seeds of stacks from previous steps are clustered with the seeds of stacks from other clades. Finally, matches to the seeds at each hierarchical step are reconstructed to build the full stack. A minimum cluster size can be set for each iteration to further increase speed at the cost of accuracy; in the example (min2) singleton loci are removed, causing data from clade b to be lost

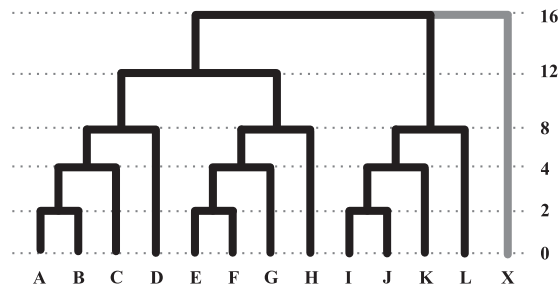


**Fig. 2.** Species tree on which RADseq data were simulated under a coalescent model. Divergence times are in coalescent units. Mutations relative to the outgroup X were sampled at different frequencies to simulate deletions in three different datasets and also to simulate disruption of the restriction recognition site in one dataset

### 2.3 Simulations

Sequence data were simulated on a species tree with 12 ingroup samples and one outgroup sample (Fig. 2) under a coalescent model within the Python package Egglib (Mita and Siol, 2012). Effective population size (50 000) and per base mutation rate ( $7 \times 10^{-9}$ ) were constant across taxa, with the deepest divergence at 16 coalescent units. I simulated 10 K loci for each of the 12 ingroup taxa at 20× coverage, with two alleles sampled from one diploid sample at 10× depth each. Reads were trimmed to 100 bp and a 6 bp barcode and 5 bp restriction recognition site were attached. Indels were introduced by sampling SNPs in the 12 ingroup taxa relative to the outgroup taxon at a probability of 0.0, 0.02 or 0.05, converting the derived allele into a deletion. This yielded three datasets that I refer to as the noIndel, lowIndel and highIndel datasets.

A larger dataset was also simulated on the same species tree to demonstrate the efficiency of the hierarchical clustering approach. In this case, 500 K loci were generated with no indels but allowing locus dropout through mutations that arise in a restriction recognition site relative to the outgroup. For this, I used a large region as the recognition site to create significant amounts of missing data between samples as expected in a deeply divergent phylogenetic dataset. This led to a dataset where each individual sample contained only ~150 K loci, but for which the total dataset comprised 500 K loci potentially shared across samples. Thus, the within-sample clustering step is relatively fast, whereas the across-sample clustering is much more computationally intensive, and benefits from the use of the hierarchical clustering. I refer to this as the noIndel-m dataset.

All simulated datasets were compared using *PyRAD* v.1.621 and *Stacks* v.1.08. To the extent possible I used analogous parameters settings for both programs. For example, the clustering threshold of 85% in *PyRAD* is equivalent to 15 base differences in *Stacks* (parameters -m6, -M13, -N15, -n15) given read lengths of 100 bp. A minimum stack depth of six was used in all analyses. Paralog filtering was not implemented on simulated data. The large noIndel-m dataset was run with the same parameter settings, but was additionally run in *PyRAD* using a two-step hierarchical clustering approach. This first clustered loci within each of the three large four-taxon clades then excluded any loci not shared across all four taxa within the clade, before subsequently clustering loci across clades.

### 2.4 Empirical data

A published RADseq dataset from Eaton and Ree (2013) was downloaded from the NCBI sequence read archive (SRA072507). It includes data from 13 closely related taxa in the flowering plant genus *Pedicularis* sequenced with Illumina GAIIx, yielding 69 bp single end reads with barcodes and restriction sites removed. In contrast to the small simulated datasets that exhibit locus dropout due to bioinformatic errors alone, the

empirical data have missing sequences owing to additional factors such as disruption to restriction sites and variation in sequencing coverage. It also contains low quality base calls and paralogs that must be filtered, making a comparison of *PyRAD* versus *Stacks* more difficult for this analysis.

To control for differences in how the two programs apply such filters, initial quality filtering was implemented only in *PyRAD*, with the resulting sequences analyzed by both programs. *Stacks* has fewer explicit filters to detect paralogs, but the closest approximations were used, and I report the results with and without paralog filters applied. The default parameters in *PyRAD* (maxHaplos=2, maxH=3, maxSharedH=3) were closely matched by using the following parameters, or manual edits, in *Stacks*, respectively: allowing only two haplotypes in a locus (-max\_locus\_stacks=2), removing loci from the final catalog if they contain more than four heterozygous sites and removing stacks from the catalog if more than three samples are heterozygous for the same site. A clustering threshold of 85% was implemented in *PyRAD*, equivalent to 10 base differences in *Stacks* (parameters -m2, -M8, -N10, -n10) given the read lengths.

Detailed parameter settings and scripts to reproduce all simulated and empirical analyses are available as an IPython Notebook in the Supplementary Materials. Statistics measuring the distribution of taxon coverage across each assembled dataset were measured from the results of each analysis found in either the '.haplotypes.tsv' output of *Stacks* or in the '.stats' output of *PyRAD*. Run times were also compared, where each analysis was run separately on a Linux machine with 24 3.47 GHz Intel Xeon processors, using 12 parallel processes in *PyRAD* or 12 threads in *Stacks*.

## 3 RESULTS

### 3.1 Simulation results

For the three small simulated datasets both *Stacks* and *PyRAD* retained all reads through the de-multiplexing and initial filtering steps. Similarly, within-sample clustering accurately recovered all 10 K stacks for each taxon when either program analyzed the noIndels dataset. In the lowIndels and highIndels datasets, *PyRAD* performed nearly identically, recovering an average of 10 000.0 and 10 000.2 consensus sequences per sample, respectively, whereas *Stacks* recovered an average of 10 027.4 and 10 087.4 consensus sequences per sample, a result of splitting loci that are polymorphic for one or more indels within a sample.

The effect of indels is more pronounced when clustering across samples, where RAD sequences are more likely to exhibit indel variation. *PyRAD* recovered 10 001, 10 003 and 10 086 loci in the three datasets with increasing proportions of indels, while *Stacks* recovered 10 000, 12 226 and 16 285, respectively. Because only 10 000 loci were simulated, those recovered beyond this number represent the splitting of loci caused by a failure to identify homology. Levels of sequence divergence are equal across the three datasets because indels were introduced by replacing mutations—meaning their phylogenetic distribution is identical to that of other mutations—thus, the different results represent the effect of indel variation alone.

*PyRAD* identifies homology almost equally across the three datasets (Fig. 3), whereas *Stacks* performs worse when the data contain more indels, to the point of splitting nearly half the loci in the highIndels dataset into multiple loci shared by fewer taxa. This led to lower average taxon coverage per locus in the assembled *Stacks* datasets, as well as fewer loci with full coverage across all taxa (Table 1). In all three small simulated datasets the

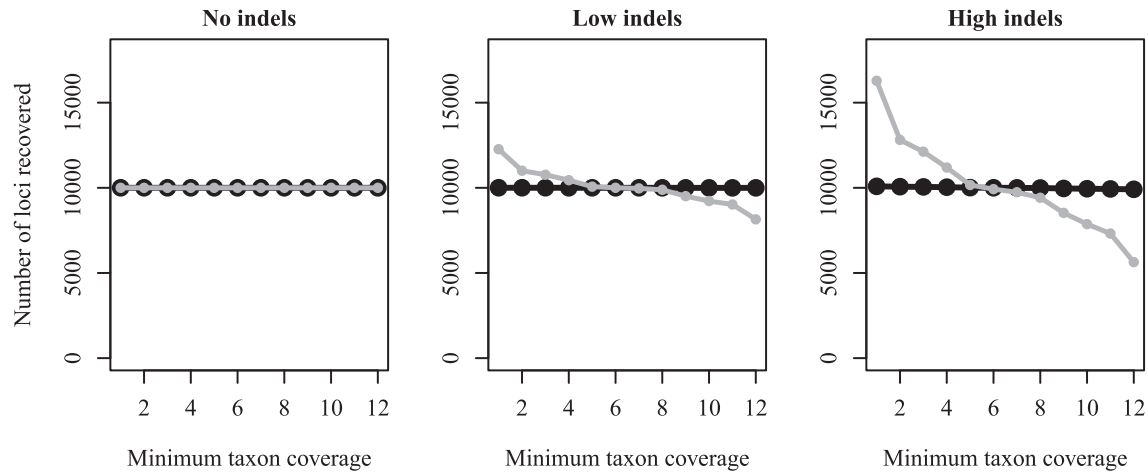


**Fig. 3.** Comparison of *PyRAD* (black circles) versus *Stacks* (gray circles) in assembling simulated RADseq datasets that differ in their amount of indel variation. The two programs perform identically in the absence of indels (no indels), but in the presence of indels (low indels and high indels), *Stacks* splits loci with indel variation into multiple loci with lower taxon coverage. Meaning a greater number of loci are shared across fewer taxa. *PyRAD*, in contrast, is little affected by indels and recovers higher taxon coverage across all indel-containing datasets

**Table 1.** Comparison of *PyRAD* and *Stacks* in assembling simulated and empirical RADseq datasets of different sizes (Ntaxa & Nloci) and with different proportions of indels

Data	Ntaxa	Nloci	Software	Avg.cov	%Full.cov	Time
noIndel	12	10 K	<i>PyRAD</i>	12.0	100.0	0.31
noIndel	12	10 K	<i>Stacks</i>	12.0	100.0	0.62
lowIndel	12	10 K	<i>PyRAD</i>	12.0	100.0	0.34
lowIndel	12	10 K	<i>Stacks</i>	9.8	81.5	0.65
highIndel	12	10 K	<i>PyRAD</i>	11.9	99.1	0.32
highIndel	12	10 K	<i>Stacks</i>	7.4	56.3	0.70
noIndel-m	12	500 K	<i>PyRAD</i>	4.5	0.1	10.47
noIndel-m	12	500 K	<i>PyRAD*</i>	2.9	0.1	2.95
noIndel-m	12	500 K	<i>Stacks</i>	4.5	0.1	25.70
empirical	13	178 K	<i>PyRAD</i>	3.0	1.4	36.42
empirical	13	207 K	<i>Stacks</i>	2.7	0.9	79.25
empirical-p	13	181 K	<i>PyRAD</i>	2.9	1.1	36.42
empirical-p	13	214 K	<i>Stacks</i>	2.4	0.5	79.25

*Note:* Performance is measured as the average number of samples recovered per locus (Avg.cov) and percentage of Nloci with data recovered from all samples in Ntaxa (%Full.cov). The noIndel-m and empirical datasets experience locus dropout from mutations to restriction sites, and the latter also from variable quality and sequencing coverage. Run times (hours) are compared for assemblies using 12 processors. When hierarchical clustering was implemented in *PyRAD* (\*) with a minimum coverage of four, it greatly reduced run times while still retaining all full coverage loci. Empirical results are shown with paralog filters applied (-p) and without. The number of recovered loci (Nloci) was used to calculate %Full.cov.

*PyRAD* analysis finished in approximately half the time of *Stacks*.

**3.1.1 Large hierarchical clustering results** Both programs recovered similar results for the large noIndel-m dataset in terms of average taxon coverage and number of loci shared across all taxa (Table 1). *Stacks* took >25 h to run, while *PyRAD* finished in about half that time. Hierarchical clustering in *PyRAD*

improved speed significantly, reducing the run time to less than 3 h, but at the cost of reducing the average taxon coverage across the dataset by one-third. However, it had no effect on the percentage of loci recovered across all taxa, as the data that were excluded during hierarchical clustering represent loci shared by few samples. For large datasets that include many sampled individuals and large numbers of loci, the dramatic reduction in run times achieved through this approach will be useful.

### 3.2 Empirical results

When assembled by *PyRAD* the empirical dataset recovered 181 289 loci of which 56.4% were singletons, but for which >43 K had taxon coverage of four or more, and 2465 were recovered across all taxa. In comparison, *Stacks* recovered 213 742 loci with a greater proportion of singletons (59.4%) and only 1940 loci shared across all taxa (Table 1). This difference is more striking after applying paralog filters to both analyses, wherein *PyRAD* recovers 1989 loci across all taxa but *Stacks* recovers only 1123. Overall, *PyRAD* recovered more loci at high taxon coverage and fewer loci at low coverage than *Stacks* (Fig. 4). In contrast to the simulated datasets, these results show clearly that locus dropout is a true feature of empirical data regardless of the bioinformatic method used. We should not expect to recover 100% of data across samples, especially when they are highly divergent, but to the extent homology is present among sequences in the dataset, I show here that *PyRAD* has greater ability to detect it.

In the minimally phylogenetic informative dataset (taxon coverage greater than three) from the paralog filtered empirical *PyRAD* output, 32% of loci contained at least one indel, and of the loci with full taxon coverage, 15% contained indels. Comparing these values to the frequency of indels in the small simulated datasets, where 21 and 48% of loci contained indels (for the lowIndels and highIndels datasets, respectively) shows that the simulated values represent realistic proportions of indel



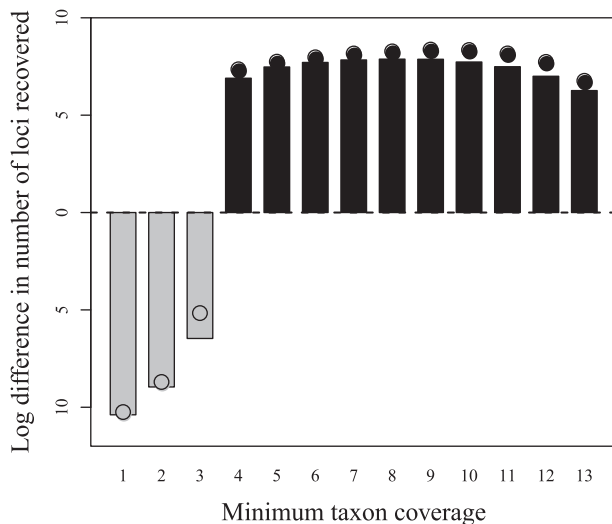


**Fig. 4.** The log difference in number of loci recovered at each level of taxon coverage from the empirical RADseq dataset of Eaton and Ree (2013) when analyzed by *PyRAD* and *Stacks*. Below the center line, *Stacks* recovered more loci (gray), while above the line, *PyRAD* recovered more (black). Circles indicate the comparison on data not filtered for paralogs and the bars after filtering for paralogs. *PyRAD* recovered more loci shared across a greater number of taxa, making its assembled dataset more phylogenetically informative

variation as expected across a similar sized dataset at a shallow phylogenetic scale.

## 4 DISCUSSION

### 4.1 RADseq at the phylogenetic scale

One of the greatest barriers to RADseq phylogenetics stems from the significant amounts of missing data that are expected to result from mutations to restriction recognition sites. However, no empirical studies have yet shown whether this form of locus dropout is in fact the primary source of missing data. Instead, insufficient sequencing coverage and a failure to identify homology during bioinformatic analyses may account for a significant proportion of locus dropout, particularly in studies at shallow phylogenetic scales. Here I show that *PyRAD* performs better than the current *de facto* alternative software for assembling RADseq datasets from divergent samples that include realistic proportions of indel variation.

Indel variation is common even within a single species (Mullaney *et al.*, 2010), and thus, it should be no surprise that restriction-site-associated libraries often sample regions containing such variation. Within repetitive DNA elements (i.e. simple sequence repeats, microsatellites), indels can arise rapidly through slipped-strand mispairing during DNA replication (Levinson and Gutman, 1987), giving rise to single or often tandem repeat nucleotide differences between taxa. While it is typically desirable to exclude large repetitive genomic regions from phylogenetic analyses (attempted by *pyRAD* within the framework of ‘paralog filtering’), the probability any locus contains at least a single or few short repeat bases is high. Rather than excluding or splitting loci that differ by short repeats,

accurately clustering and aligning them across disparate species will help to create more complete and phylogenetically informative datasets.

### 4.2 Options and extensions

**4.2.1 Paired-end reads and sequence overlap** *PyRAD* uses two methods that greatly improve the speed and quality of paired-end library assemblies. The first is specific to paired ddRAD libraries for which first and second reads are subtended by different restriction enzyme cut sites. Here, first and second reads can either be analyzed separately and treated as unlinked loci (ddRAD method), concatenated and treated as long contigs (concatenated ddRAD method) or clustered by only their first reads but with second read data kept associated with first read clusters (split ddRAD method). The first approach loses information about linkage of the paired reads. The second method retains this information, but requires greater computation because of longer read lengths, while the third, ‘split ddRAD clustering’, offers a dramatic speed improvement over clustering longer concatenated reads while also retaining linkage information. It also allows assembling more highly divergent second reads, which often contain low-quality base calls.

The second feature *PyRAD* offers for paired-end data is the ability to identify partial overlap among sequences. This proves particularly useful for paired-end ddRAD or GBS libraries that suffer from variable size selection, which can result in overlap among paired-end reads or between single-end reads sequenced from either end of short GBS fragments. Using reverse complement clustering, contigs are constructed from overlapping regions with sufficient coverage to make consensus base calls. This allows building contigs longer than individual read lengths and increases quality by combining sequences with high-quality base reads at either end. Most importantly, it reduces duplication that would result from treating partially overlapping reads as separate loci.

**4.2.2 Introgression analyses** *PyRAD* is being developed to include a number of analysis tools in addition to data assembly. This currently includes measurement of D-statistics (Durand *et al.*, 2011) and related tests for genomic introgression (Eaton and Ree, 2013). For this, *PyRAD* uses the distribution of RADseq markers as putatively unlinked loci and performs non-parametric bootstrapping. A number of options are available to optimize the amount of shared data across samples when performing these tests, including SNP-based tests and averaging allele counts across multiple sampled individuals.

## 5 CONCLUSION

*PyRAD* performs *de novo* assembly of RADseq datasets, including RAD, GBS, ddRADseq and paired-end options. It is designed to perform equally well from population to phylogenetic scales and is currently being implemented across this range, from linkage analyses among siblings to clade-level phylogenies with hundreds of tips. A major goal of this software was ease of use, and for this reason, it uses common file formats familiar to those working in phylogenetics and offers a variety of output formats for downstream analyses, from SNP and allelic data to individual

or concatenated loci. Because the software does not need to be compiled, PyRAD is easy to install on any desktop or computing cluster. It does not require large memory usage, and an analysis can be easily split into multiple shorter-length jobs through its step-wise execution.

## ACKNOWLEDGEMENT

Many thanks to R. Ree, B. Rubin, A. Hipp, M. Escudero and K. Ramanauskas for motivating the development of PyRAD, helping to identify bugs and for their many suggestions. Thanks also to R. Edgar whose software underlies much of this program and to two anonymous reviewers for improvements to the manuscript.

**Funding:** This research was supported by a National Science Foundation Dissertation Improvement Grant (DEB-1110598).

**Conflict of Interest:** none declared.

## REFERENCES

- Baird, N. *et al.* (2008) Rapid SNP discovery and genetic mapping using sequenced RAD markers. *PLoS One*, **3**, e3376.
- Bergey, C. *et al.* (2013) A new method for genome-wide marker development and genotyping holds great promise for molecular primatology. *Int. J. Primatol.*, **34**, 303–314.
- Cariou, M. *et al.* (2013) Is RAD-seq suitable for phylogenetic inference? An *in silico* assessment and optimization. *Ecol. Evol.*, **3**, 846–852.
- Catchen, J. *et al.* (2013) Stacks: an analysis tool set for population genomics. *Mol. Ecol.*, **22**, 31243140.
- Catchen, J. M. *et al.* (2011) Stacks: building and genotyping loci de novo from short-read sequences. *G3*, **1**, 171–182.
- Chong, Z. *et al.* (2012) Rainbow: an integrated tool for efficient clustering and assembling RAD-seq reads. *Bioinformatics*, **28**, 2732–2737.
- Durand, E. Y. *et al.* (2011) Testing for ancient admixture between closely related populations. *Mol. Biol. Evol.*, **28**, 2239–2252.
- Eaton, D. A. R. and Ree, R. H. (2013) Inferring phylogeny and introgression using RADseq data: an example from flowering plants (Pedicularis: Orobanchaceae). *Syst. Biol.*, **62**, 689–706.
- Edgar, R. C. (2004) MUSCLE: multiple sequence alignment with high accuracy and high throughput. *Nucleic Acids Res.*, **32**, 1792–1797.
- Edgar, R. C. (2010) Search and clustering orders of magnitude faster than BLAST. *Bioinformatics*, **26**, 2460–2461.
- Etter, P. *et al.* (2011) Local *de novo* assembly of RAD paired-end contigs using short sequencing reads. *PLoS One*, **6**, e18561.
- Jones, J. C. *et al.* (2013) The evolutionary history of xiphophorus fish and their sexually selected sword: a genome-wide approach using restriction site-associated dna sequencing. *Mol. Ecol.*, **22**, 2986–3001.
- Keller, I. *et al.* (2013) Population genomic signatures of divergent adaptation, gene flow and hybrid speciation in the rapid radiation of lake victoria cichlid fishes. *Mol. Ecol.*, **22**, 2848–2863.
- Levinson, G. and Gutman, G. A. (1987) Slipped-strand mispairing: a major mechanism for DNA sequence evolution. *Mol. Biol. Evol.*, **4**, 203–221.
- Lexer, C. *et al.* (2013) Next generation biogeography: towards understanding the drivers of species diversification and persistence. *J. Biogeogr.*, **40**, 1013–1022.
- Li, H. *et al.* (2008) Mapping short DNA sequencing reads and calling variants using mapping quality scores. *Genome Res.*, **18**, 1851–1858.
- Lynch, M. (2008) Estimation of nucleotide diversity, disequilibrium coefficients, and mutation rates from high-coverage genome-sequencing projects. *Mol. Biol. Evol.*, **25**, 2409–2419.
- Mita, S. D. and Siol, M. (2012) EggLib: processing, analysis and simulation tools for population genetics and genomics. *BMC Genet.*, **13**, 27.
- Mullaney, J. M. *et al.* (2010) Small insertions and deletions (INDELs) in human genomes. *Hum. Mol. Genet.*, **19**, R131–R136.
- Nadeau, N. J. *et al.* (2013) Genome-wide patterns of divergence and gene flow across a butterfly radiation. *Mol. Ecol.*, **22**, 814–826.
- Narum, S. R. *et al.* (2013) Genotyping-by-sequencing in ecological and conservation genomics. *Mol. Ecol.*, **22**, 2841–2847.
- Peterson, B. K. *et al.* (2012) Double digest RADseq: an inexpensive method for *de novo* SNP discovery and genotyping in model and non-model species. *PLoS One*, **7**, e37135.
- Rubin, B. E. R. *et al.* (2012) Inferring phylogenies from RAD sequence data. *PLoS One*, **7**, e33394.
- Stölting, K. N. *et al.* (2013) Genomic scan for single nucleotide polymorphisms reveals patterns of divergence and gene flow between ecologically divergent species. *Mol. Ecol.*, **22**, 842–855.
- The Heliconius Genome Consortium. (2012) Butterfly genome reveals promiscuous exchange of mimicry adaptations among species. *Nature*, **487**, 94–98.
- Wagner, C. E. *et al.* (2013) Genome-wide RAD sequence data provide unprecedented resolution of species boundaries and relationships in the lake victoria cichlid adaptive radiation. *Mol. Ecol.*, **22**, 787–798.
- Wang, X. Q. *et al.* (2013) Identification of SNP markers for inferring phylogeny in temperate bamboos (Poaceae: Bambusoideae) using RAD sequencing. *Mol. Ecol. Resour.*, **13**, 938–945.